Am J Physiol Endocrinol Metab 293: E713–E725, 2007.
First published June 19, 2007; doi:10.1152/ajpendo.00194.2007.

Macrophage TNF-α contributes to insulin resistance and hepatic steatosis in diet-induced obesity

Bart M. De Taeye,[1] Tatiana Novitskaya,[1] Owen P. McGuinness,[2] Linda Gleaves,[1] Mousumi Medda,[1] Joseph W. Covington,[1] and Douglas E. Vaughan[1]

Departments of [1]Medicine and [2]Molecular Physiology and Biophysics, Vanderbilt University, Nashville, Tennessee

Submitted 29 March 2007; accepted in final form 15 June 2007

De Taeye BM, Novitskaya T, McGuinness OP, Gleaves L, Medda M, Covington JW, Vaughan DE. Macrophage TNF-α contributes to insulin resistance and hepatic steatosis in diet-induced obesity. *Am J Physiol Endocrinol Metab* 293: E713–E725, 2007. First published June 19, 2007; doi:10.1152/ajpendo.00194.2007.—Obesity is commonly associated with development of insulin resistance and systemic evidence of inflammation. Macrophages contribute to inflammatory amplification in obesity and may contribute directly to insulin resistance and the development of nonalcoholic fatty liver disease through the production of inflammatory cytokines, including tumor necrosis factor (TNF)-α. To test this hypothesis, we transplanted male wild-type (WT) and TNF-α deficient (KO) mice with either TNF-α-sufficient (TNF-$\alpha^{+/+}$) or TNF-α-deficient (TNF-$\alpha^{-/-}$) bone marrow. After consuming a high-fat diet for 26 wk, metabolic and morphometric characteristics of the animals were analyzed. While there were no differences in terms of relative weight gain, body composition analysis yielded a lower relative adipose and higher relative lean mass in mice lacking TNF-α, which was partially explained by reduced epididymal fat pad and liver weight. TNF-$\alpha^{-/-}$→KO mice exhibited enhanced insulin sensitivity compared with that observed in TNF-$\alpha^{+/+}$→KO mice; remarkably, no protection against insulin resistance was provided by transplanting TNF-$\alpha^{-/-}$ bone marrow in WT mice compared with TNF-$\alpha^{+/+}$→WT. The preserved insulin sensitivity seen in TNF-$\alpha^{-/-}$→KO mice provided protection against the development of hepatic steatosis. Taken together, these data indicate that macrophage-derived TNF-α contributes to the pattern and extent of fat accumulation and insulin resistance in diet-induced obesity; however, this contribution is negligible in the presence of host-derived TNF-α.

cytokine; inflammation; hyperinsulinemic-euglycemic clamping

OBESITY IS AN INCREASINGLY important public health issue. Visceral obesity has been defined as an important element of the metabolic syndrome, and expansion of the visceral fat mass coupled with disturbed metabolic profile has been shown to contribute to the development of obesity complications such as insulin resistance and nonalcoholic fatty liver disease (NAFLD). The development of obesity coincides with a significant increase of bone marrow-derived macrophage infiltration in adipose tissue, associated with the expression of inflammatory cytokines, considered to be responsible for the majority of the obesity complications (6, 7, 32, 47, 48).

The proinflammatory cytokine tumor necrosis factor-α (TNF-α) has been studied extensively for effects on the regulation of adipocyte differentiation, lipid metabolism, and insulin sensitivity. TNF-α has been demonstrated to contribute to the development of insulin resistance in a variety of experimental models of obesity (17–21, 29, 35, 44–46). In humans, TNF-α expression levels are positively linked with insulin resistance and other cardiovascular risk factors (17, 24, 49). Multiple mechanisms have been suggested to account for these metabolic effects of TNF-α (reviewed in Refs. 15 and 29).

Although originally believed to originate exclusively from macrophages (2, 42), more recent evidence suggests that TNF-α is produced by adipocytes as well as by monocytes and macrophages, and circulates in increased levels in individuals with obesity (15, 16, 34). Expression analysis of macrophage and nonmacrophage cell populations isolated from adipose tissue indicates that adipose tissue macrophages are responsible for almost all adipose tissue TNF-α expression (7, 47). However, in lean mice, the adipocyte is one of the primary cell types responsible for the production of TNF-α by adipose tissue, which might be explained by the fact that lean adipose tissue contains considerably fewer macrophages than obese adipose tissue (7, 47).

In the liver, Kupffer cells are the primary source of hepatic TNF-α (40) and have been shown to be recruited and activated in a nutritional model of nonalcoholic steatohepatitis (NASH; see Ref. 41). TNF-α is thought to regulate Kupffer cell activation through both autocrine and paracrine mechanisms (23). Recently, it was shown that TNF-α receptor-deficient mice are protected from liver steatosis and show a decrease in activated Kupffer cells (41). Furthermore, treatment with anti-TNF-α antibodies improves NAFLD in *ob/ob* mice (26).

To analyze the impact of TNF-α produced by bone marrow-derived cells (e.g., macrophages), on the development of insulin resistance and NAFLD in the setting of diet-induced obesity, we transplanted both WT and KO mice with either TNF-α-sufficient (TNF-$\alpha^{+/+}$) or TNF-α-deficient (TNF-$\alpha^{-/-}$) marrow. The results indicate that TNF-α originating from bone marrow-derived cells influences diet-induced insulin resistance and NAFLD in TNF-$\alpha^{-/-}$ animals. However, the impact and effects are not restricted to marrow-derived TNF-α.

MATERIALS AND METHODS

Animal procedures. Wild-type B6;129SF2/J littermates [TNF-$\alpha^{+/+}$, wild type (WT)] and TNF-α-deficient littermates [TNF-$\alpha^{-/-}$, knockout (KO)] aged 4–5 wk on a B6;129S6/J background were purchased from the Jackson Laboratory (Bar Harbor, ME). Mice were housed in a pathogen-free barrier facility (12:12-h light-dark cycle). When the mice were 8–9 wk old, the study was started. Two weeks before and 2 wk following the actual performance of the bone marrow transplantation, 100 mg/l neomycin and 10 mg/l polymyxin B sulfate (both

Address for reprint requests and other correspondence: D. E. Vaughan, Vanderbilt Univ. Medical Center, Dept. of Medicine, Division of Cardiovascular Medicine, 383 Preston Research Bldg., Nashville, TN 37232 (e-mail: Douglas.e.vaughan@vanderbilt.edu).

The costs of publication of this article were defrayed in part by the payment of page charges. The article must therefore be hereby marked "*advertisement*" in accordance with 18 U.S.C. Section 1734 solely to indicate this fact.

from Sigma-Aldrich, St. Louis, MO) were added to the acidified water (pH 2.6). Bone marrow was collected from donor mice by flushing femurs and tibia with RPMI 1640 media (Invitrogen, Carlsbad, CA) containing 2% FBS and 5 U/ml heparin (Sigma-Aldrich). Bone marrow cells were washed, resuspended in fresh media, and counted. Recipient mice were lethally irradiated (9 Gy), and 4 h later, 2–5 × 10^6 marrow cells in 0.2 ml were transplanted by retroorbital venous plexus injection. By design, male TNF WT and KO mice received either WT (TNF-$\alpha^{+/+}$) or KO (TNF-$\alpha^{-/-}$) bone marrow ($n = 10$ for each of the four groups). The success of the deletion of the original bone marrow and the uptake of the received donor bone marrow were assessed by analysis of the bone marrow cells of the recipient mice after death (see further). After the recovery period of 2 wk, mice were placed on a high-fat diet [HFD; time (t) = 0 wk; diet TD 88137; Harlan Teklad Madison, WI] in which 42% of total calories are derived from fat for 26 wk. A similar diet has been shown to induce obesity in mice with a C57BL/6 × 129 genetic background (45). Body weights were measured every 2 wk. Food intake was determined three times (at 4, 10, and 20 wk) during the 26 wk on the HFD for the individual mice, each time over a 24-h period, and expressed as kilocalories per mouse per day. After daytime food withdrawal (6 h), venous blood was obtained from the mice by retroorbital sinus puncture using a tube with anticoagulant (ammonium heparin), before switching to the HFD ($t = 0$ wk), and after 12 wk on the HFD. The plasma was isolated by centrifugation at 3,000 *g* for 15 min and stored at −80°C. No plasma was collected at the end of the 26 wk on HFD to minimize the risk of losing animals in the hyperinsulinemic-euglycemic clamp studies. Fasting glucose levels were determined using a HemoCue glucose monitor (HemoCue, Ängelholm, Sweden). After 25 wk on the HFD, body composition of unanesthetized mice was determined using a Minispec model mq 7.5 (7.5 mHz; Bruker Optics, Billerica, MA) together with indirect calorimetry studies as described below. After 26 wk on the HFD, the mice underwent surgeries in groups of three (randomized over the 4 'gene combinations'), followed 5 days later by the metabolic studies described below. White adipose tissue, heart, liver, spleen, kidneys, pancreas, hindlimb muscle, and bone marrow were harvested. Liver, heart, pancreas and white adipose tissue were weighed. One portion of each organ was snap-frozen in liquid nitrogen and stored at −80°C for RNA extraction or frozen sections for immunohistochemistry; other portions were used for histology and immunohistochemistry. All animal protocols were approved by the Vanderbilt University Institutional Animal Care and Use Committee.

Indirect calorimetry. Oxygen consumption ($\dot{V}O_2$) and the respiratory exchange ratio were measured by an Oxymax indirect calorimeter (Columbus Instruments, Columbus, OH) with an air flow of 0.6 l/min. $\dot{V}O_2$ is expressed as the volume of O_2 consumed per kilogram lean body weight per hour. Following a 1 h adaptation period in the metabolic chamber, $\dot{V}O_2$ was measured, starting at 10:00 A.M., in individual mice for 1 min at 25-min intervals for a total of 20 h under a consistent environmental temperature (22°C). The respiratory exchange ratio is the ratio of the volume of CO_2 produced to the volume of O_2 consumed. Energy expenditure (EE) was calculated as $EE = (3.815 + 1.232 \times \dot{V}CO_2/\dot{V}O_2) \times \dot{V}O_2$, where $\dot{V}CO_2$ is carbon dioxide production. Mice ambulatory activity was simultaneously estimated by the number of laser beams broken in both *X* and *Y* directions.

Animal surgery and hyperinsulinemic-euglycemic clamp experiments. The euglycemic-hyperinsulinemic clamp studies were performed as described previously (1, 13) at 26 wk after the HFD in chronically catheterized conscious mice in the Mouse Metabolic Phenotyping Center at Vanderbilt University Medical Center. Briefly, catheterization of the jugular vein was carried out 5 days before study. Blood samples were obtained from the tail vein. Each animal was fasted for 5 h on the morning of the experiment (7:00 A.M.). At 10:00 A.M., the primed (10 μl/min for 2 min) continuous (1 μl/min) [3-^{3}H]glucose (50 μCi/ml saline) infusion was started. After basal sampling, a primed (40 mU/kg) continuous (4 $mU \cdot kg^{-1} \cdot min^{-1}$) insulin (Humulin R; Eli Lilly, Indianapolis, IN) infusion was started at *time 0* (12:00 P.M.) and infused for the duration of the study (145 min). [3-^{3}H]glucose infusion was increased to 2 μl/min. Blood samples (60–200 μl) were taken every 10 min from $t = 80$ to $t = 120$ min and processed to determine glucose specific activity. Insulin levels were determined from samples obtained at $t = -10$ and 120 min. Hematocrit was determined before the start of the insulin infusion and at $t = 90$ min. After the 120-min sample, a 2-[^{14}C]deoxyglucose (2-[^{14}C]DG) bolus was injected in the jugular vein (12 μCi), and blood samples were taken at 122, 125, 130, 135, and 145 min and processed to determine glucose specific activity. Insulin levels were determined in the 145-min sample. During the entire study, blood glucose levels were measured from blood samples obtained every 5–10 min from the tail vein using an Accucheck glucose analyzer (Roche Diagnostics, Indianapolis, IN). Glucose (50 g/100 ml) was infused at a variable rate to maintain clamped blood glucose levels at 190–200 mg/dl.

Processing of plasma and tissue samples. Plasma samples were deproteinized with $Ba(OH)_2$ and $ZnSO_4$, and then 2-[^{14}C]DG radioactivity was determined by liquid scintillation counting (TRI-CARB 2900TR; Packard, Meriden, CT) with Ultima Gold (Packard) as scintillant. 2-Deoxy-D-glucose 6-phosphate (2-[^{14}C]DGP) was assessed in frozen muscle, heart, epididymal fat, diaphragm, brain, and liver samples as previously described (13). The accumulation of 2-[^{14}C]DGP was normalized to tissue weight and tracer bolus in all experiments. R_g was calculated as previously described (25).

Liver glycogen content was determined on 50–100 mg of tissue as described previously (4), with minor modifications.

Liver lipids were extracted using the method of Folch et al. (12). The extracts were filtered, and lipids were recovered in the chloroform phase. Individual lipid classes were separated by thin-layer chromatography using Silica Gel 60 A plates developed in petroleum ether-ethyl ether-acetic acid (80:20:1) and visualized by rhodamine 6G. Phospholipids, diglycerides, triglycerides, and cholesteryl esters were scraped from the plates and methylated using BF_3/methanol as described by Morrison and Smith (30). The methylated fatty acids were extracted and analyzed by gas chromatography. Gas chromatographic analyses were carried out on an HP 5890 gas chromatograph equipped with flame ionization detectors, an HP 3365 Chemstation, and a capillary column (SP2380, 0.25 mm × 30 m, 0.25 μm film; Supelco, Bellefonte, PA). Helium was used as a carrier gas. The oven temperature was programmed from 160 to 230°C at 4°C/min. Fatty acid methyl esters were identified by comparing the retention times with those of known standards. Inclusion of lipid standards with odd chain fatty acids permitted quantitation of the amount of lipid in the sample. Dipentadecanoyl phosphatidylcholine (C15:0), diheptadecanoin (C17:0), trieicosenoin (C20:1), and cholesteryl eicosenoate (C20:1) were used as standards.

DNA and RNA analysis. DNA was isolated from bone marrow cells collected after killing the animals. Both hindlimbs of the mice were collected; the bone marrow was isolated by flushing femurs and tibia with 10 ml of PBS (Sigma-Aldrich). After centrifugation at 3,000 *g* for 10 min, cells were resuspended in 0.4 ml cryopreservation media (EmbryoMax; Chemicon, Temecula, CA) and stored at −80°C. DNA was isolated from 0.15 ml of the cell suspension using the Qiagen DNeasy Tissue Kit (Qiagen, Valencia, CA) following the protocol for purification of total DNA from cultured animal cells according to the manufacturer's guidelines. The bone marrow cells were genotyped using the primers and PCR cycling conditions as suggested by the Jackson Laboratory [primers for the TNF-$\alpha^{-/-}$ and the TNF-$\alpha^{+/+}$ genotype recognize part of the inserted neomycin cassette (280-bp fragment) and the deleted part of the TNF-α gene (146-bp fragment), respectively]. Promega PCR Master mix (Promega, Madison, WI) was used for the reaction mixture with 40 ng of DNA for a 25-μl reaction. Reaction products were analyzed using a 1.5% agarose gel and the 1-kb DNA ladder from Promega. Transplantation efficiency was quantified using real-time RT-PCR as described below on the

genomic DNA, isolated from the bone marrow cells. The same fragments typical for TNF-$\alpha^{-/-}$ and TNF-$\alpha^{+/+}$ amplified for the genotyping, and β_2-microglobulin as internal control, were quantified using iQ SYBR Green Supermix (Bio-Rad, Hercules, CA) on an *i*-Cycler instrument (Bio-Rad). The amount of TNF-$\alpha^{-/-}$ and TNF-$\alpha^{+/+}$ gene was calculated using the $2^{-\Delta\Delta C_T}$ (where C_T is threshold cycle) method (27) and expressed relative to the level of TNF-$\alpha^{-/-}$ in TNF-$\alpha^{-/-}$→KO and TNF-$\alpha^{+/+}$ in TNF-$\alpha^{+/+}$→WT animals, respectively.

RNA was isolated from adipose tissue, liver, and hindlimb muscle using the Qiagen RNeasy Lipid, RNeasy Mini, and RNeasy Fibrous Tissue Mini kit (Qiagen), respectively, following the manufacturer's instructions. Subsequently, the RNA was reverse-transcribed using random hexamer primers and oligo(dT) with the iScript cDNA synthesis kit (Bio-Rad) following the recommended conditions from the manufacturer. Subsequently, specific cDNA targets were amplified using iQ SYBR Green Supermix (Bio-Rad) on an *i*-Cycler instrument (Bio-Rad). β-Actin cDNA was used as an endogenous reference. Samples without cDNA were included to exclude nonspecific reactions resulting from primer interactions. Furthermore, a positive control containing cDNA for the analyzed target was included. The relative levels of mRNA were quantified using the $2^{-\Delta\Delta C_T}$ method (27).

Histology and immunohistochemistry. Tissues for immunohistochemistry were fixed in 10% neutral, phosphate-buffered formalin for 24–48 h and paraffin embedded. Subsequently, the paraffin-embedded tissues were processed in 6- μm sections. Histological sections of epididymal fat pads were stained with hematoxylin and eosin and studied under 20-fold magnification to compare adipocyte size. On five randomly selected fields from three different sections, the number of stroma cell nuclei and the number of adipocytes, based on morphological criteria, were determined, and the results were expressed as a ratio ($n = 5$). Mature adipocytes are defined as differentiated cells distended with lipid material. They contain peripherally inconspicuous nuclei. Sections of liver were stained with Mayer's hematoxylin and eosin and Masson Trichrome. Frozen liver sections (6 μm) were stained with Oil red O (Sigma-Aldrich) to detect lipid accumulation. Sections were stained for 4 h in 0.5% Oil red O in propylene glycol, followed by 3 × 1 min incubations in 85% aqueous propylene glycol. After the slides were washed in distilled water, they were dried and counterstained with Mayer's hematoxylin for 1 min. Immunohistochemistry was done on serial sections of the epididymal fat for both F4/80 and TNF-α. Goat anti-mouse TNF-α (1/50; R&D Systems, Minneapolis, MN) and rat anti-mouse F4/80 (1/50; Serotec, Raleigh, NC) were used as primary antibodies. For detection, we used ready-to-use biotinylated secondary antibodies against the appropriate IgGs in combination with ready-to-use streptavidin-horseradish peroxidase and AEC for detection (all from BioGenex, San Ramon, CA).

Statistical analysis. Statistical analysis was performed using GraphPad Prism (version 4; San Diego, CA). Data are expressed as means ± SE. Statistical significance for difference between groups was evaluated using Student's *t*-test or one- or two-way ANOVA. Values of $P < 0.05$ are considered statistically significant.

The final n for the analysis was $n \leq 8$, as specified for the individual experiments. Four animals died during the 26-wk study. Four animals gained weight until around *week 12–14* before losing body weight and showing signs of sickness. These animals were killed in agreement with Institutional Animal Care and Use Committee regulations. Real-time quantitative PCR (RT-QPCR) data are expressed relative to TNF-$\alpha^{+/+}$→WT and TNF-$\alpha^{-/-}$→KO as appropriate to investigate a bone marrow (i.e., macrophage TNF-α) effect in WT and KO hosts, respectively. Because WT animals and KO animals are littermates within the group but not between groups, and considering the small weight difference between WT and KO animals at the start of the study, this approach allowed exclusion of differences caused by the genetic background and initial weight difference.

RESULTS

Macrophage TNF-α contributes significantly to adipose and liver TNF-α production. The success of the bone marrow transplantation was qualitatively analyzed by genotyping the bone marrow cells after death of the transplanted animals. Using the primers as described by the Jackson Laboratory, a 146-bp and a 280-bp PCR product is typical for TNF-$\alpha^{+/+}$ and TNF-$\alpha^{-/-}$, respectively (see MATERIALS AND METHODS). Figure 1*A* shows the results for two mice of each group. Analysis of bone marrow DNA from TNF-$\alpha^{-/-}$→KO and TNF-$\alpha^{-/-}$→WT mice generated a 280-bp fragment as expected, indicating the presence of the KO marrow and eradication of WT cells for the second group. The 146-bp fragment seen for TNF-$\alpha^{+/+}$→WT and TNF-$\alpha^{+/+}$→KO confirmed the WT bone marrow uptake. However, for the latter group, a 280-bp fragment was present indicating that the KO bone marrow was not completely eradicated. Analysis of the bone marrow from the other mice showed the same pattern as shown in Fig. 1*A* (data not shown). To quantify the transplantation efficiency, genomic DNA isolated from the bone marrow cells was used for RT-QPCR, allowing the

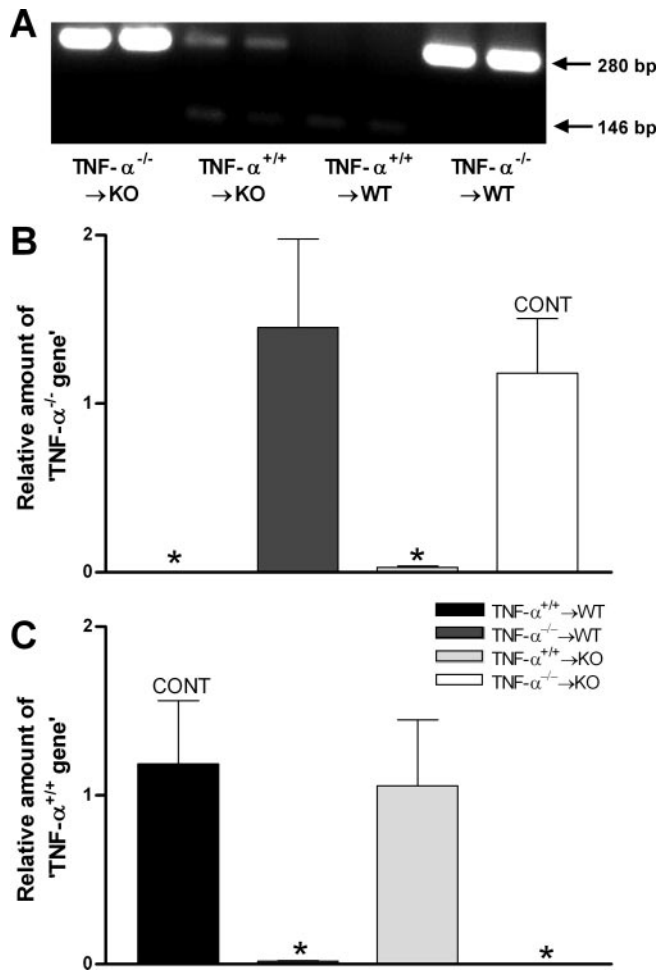

Fig. 1. Efficiency of the bone marrow transplantation. *A*: SDS-PAGE revealed a 280-bp and/or 146-bp fragment typical for tumor necrosis factor (TNF)-α deficiency and presence, respectively. *B* and *C*: quantification of the TNF-α-deficient (TNF-$\alpha^{-/-}$) and TNF-α-sufficient (TNF-$\alpha^{+/+}$) gene in the respective groups. WT, wild type; KO, knockout. Data are expressed as means ± SE. *$P < 0.05$ vs. control (CONT); $n = 7–8$ experiments.

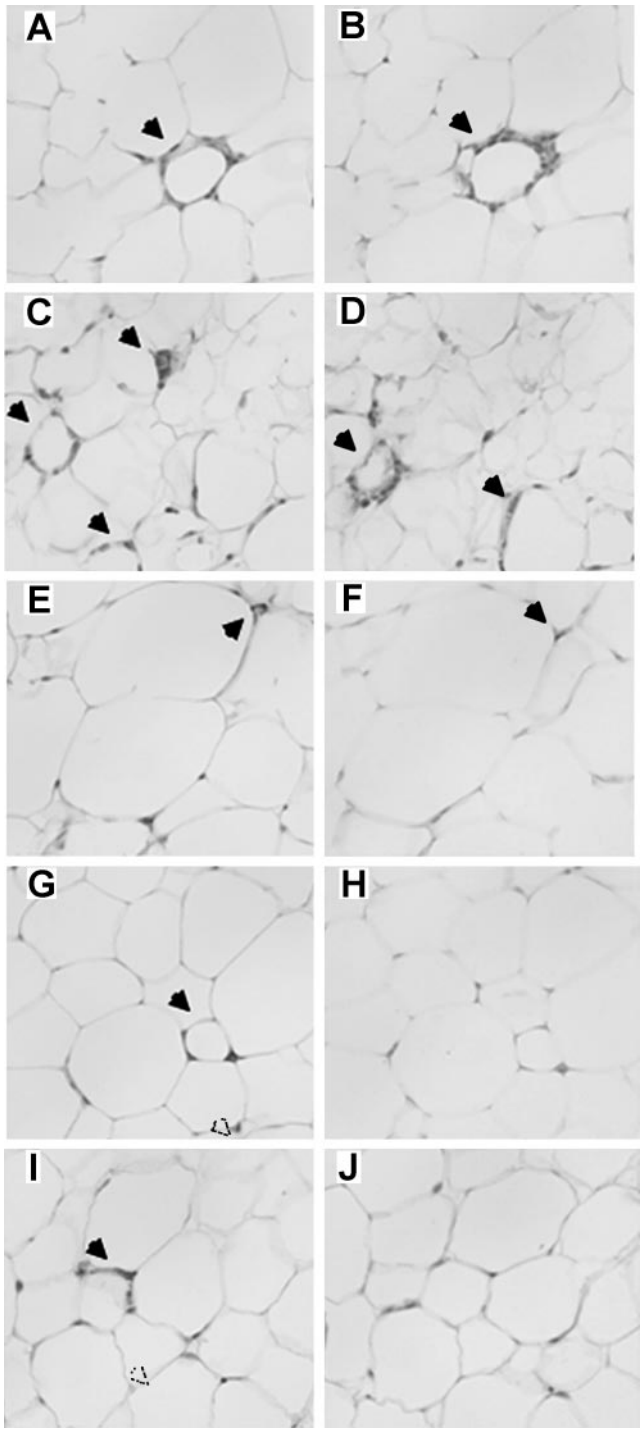

Fig. 2. Obesity development is associated with macrophage recruitment from the bone marrow. Serial epididymal fat pad sections from TNF-$\alpha^{+/+}$→WT (*A* and *B*), TNF-$\alpha^{-/-}$→WT (*C* and *D*), TNF-$\alpha^{+/+}$→KO (*E–H*), and TNF-$\alpha^{-/-}$→KO (*I* and *J*) animals are shown stained for F4/80 (*A*, *C*, *E*, *G*, and *I*) and TNF-α (*B*, *D*, *F*, *H*, and *J*).

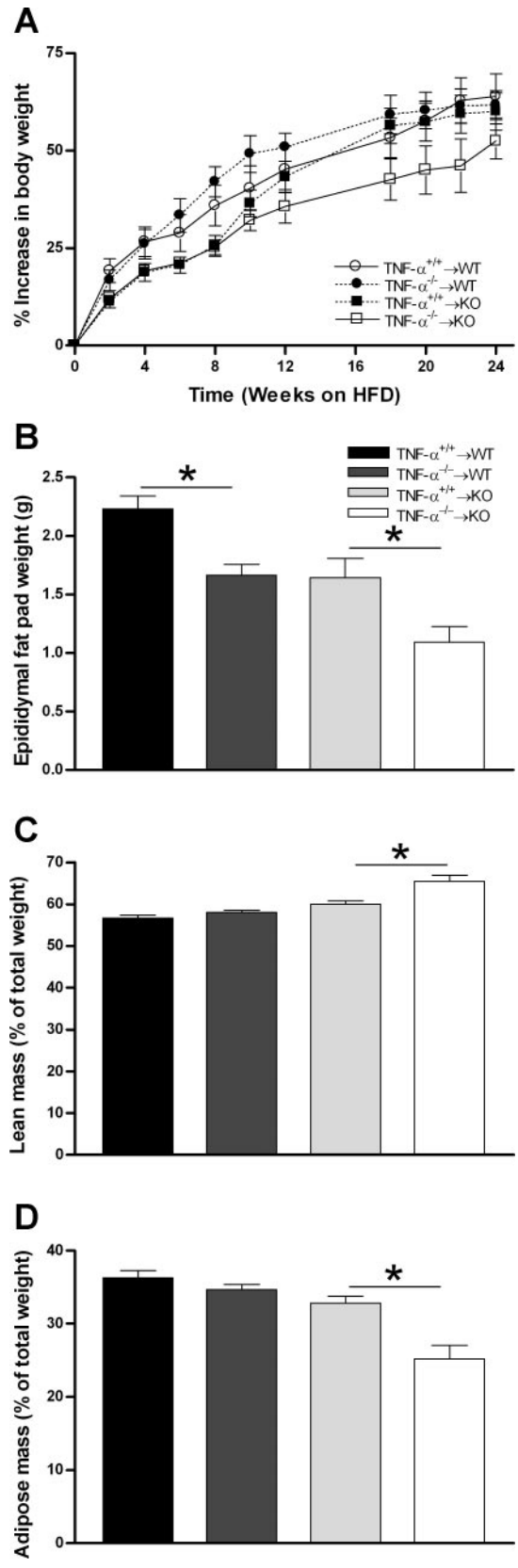

Fig. 3. Macrophage TNF-α influences obesity development. Whereas relative weight gain did not differ (*A*), epididymal fat pad weight varied significantly (*$P < 0.05$; *B*), in agreement with relative lean mass (*$P = 0.004$; *C*) and relative adipose mass (*$P = 0.004$; *D*). Data are expressed as means ± SE; $n = 7–8$.

quantification of the 146-bp (TNF-$\alpha^{+/+}$) and 280-bp (TNF-$\alpha^{-/-}$) fragment for each animal ($n = 7–8$). The amount of the TNF-$\alpha^{-/-}$-specific fragment (Fig. 1*B*) and the TNF-$\alpha^{+/+}$-specific fragment (Fig. 1*C*) was calculated relative to the amount of this fragment in the TNF-$\alpha^{-/-}$→KO and TNF-$\alpha^{+/+}$→WT animals, respectively. The results indicate that the TNF-$\alpha^{+/+}$-spe-

Table 1. *Weights before and after high-fat diet for 26 wk*

Genotype	Week 0		Week 26	
	Weight, g	*P*	Weight, g	*P*
TNF-$\alpha^{+/+}$→WT	26.8±0.8	0.40	42.4±1.2	0.78
TNF-$\alpha^{-/-}$→WT	27.2±1.1		42.9±1.5	
TNF-$\alpha^{+/+}$→KO	23.5±0.4	0.27	37.0±1.1	0.24
TNF-$\alpha^{-/-}$→KO	22.3±1.0		34.7±1.5	

Values are expressed as means ± SE; n = 7–8 experiments. TNF-$\alpha^{-/-}$, tumor necrosis factor-α (TNF-α) sufficient; TNF-$\alpha^{-/-}$, TNF-α deficient; WT, wild type; KO, knockout. *P* values are for the comparison as indicated in the table.

cific fragment is as abundant in the TNF-$\alpha^{+/+}$→KO as in the TNF-$\alpha^{+/+}$ →WT animals (P = 0.81); in TNF-$\alpha^{-/-}$→WT animals the level is only 1.7% of that in the TNF-$\alpha^{+/+}$→WT animals (P = 0.01), and it is not present in the TNF-$\alpha^{-/-}$→KO animals (P = 0.02). Conversely, the TNF-$\alpha^{-/-}$-specific fragment is as abundant in the TNF-$\alpha^{-/-}$→WT as in the TNF-$\alpha^{-/-}$→KO animals (P = 0.67); in TNF-$\alpha^{+/+}$→KO animals the level is only 2.5% of that in the TNF-$\alpha^{-/-}$→KO animals (P = 0.008), and it is not present in the TNF-$\alpha^{+/+}$→WT animals (P = 0.03).

RT-QPCR, using oligonucleotide primers designed to amplify the sequence of the TNF-α gene deleted in the KO animals, was performed to quantify the amount of TNF-α mRNA in epididymal fat pad, liver, and hindlimb muscle (n = 7–8). When compared with TNF-$\alpha^{+/+}$→WT animals, TNF-$\alpha^{-/-}$→WT animals had 84% (1.05 ± 0.10 vs. 0.17 ± 0.05; $P < 0.0001$), 88% (1.18 ± 0.28 vs. 0.14 ± 0.05; P = 0.006), and 29% (1.15 ± 0.6 vs. 0.82 ± 0.63; P = 0.63) less TNF-α mRNA in the epididymal fat pad, liver, and hindlimb muscle, respectively. In KO hosts receiving TNF-$\alpha^{-/-}$ marrow, no TNF-α mRNA was detected; the levels in the TNF-$\alpha^{+/+}$→KO mice were greater than or equal to those seen in TNF-$\alpha^{+/+}$→WT mice for adipose tissue and liver, respectively. Muscle from TNF-$\alpha^{+/+}$→KO mice contained 63% TNF-α mRNA relative to TNF-$\alpha^{+/+}$→WT (data not shown). These data indicate that, in diet-induced obesity, macrophage TNF-α contributes significantly to the total production of TNF-α in liver and adipose tissue, the two most important organs for lipid homeostasis.

Immunohistochemical detection of TNF-α and F4/80 on serial sections indicates that, while some resident macrophages from the host are still present, the majority are donor derived, i.e., recruited from the bone marrow (Fig. 2). In adipose tissue from TNF-$\alpha^{+/+}$→WT animals, macrophages (F4/80; Fig. 2*A*) colocalize with TNF-α (Fig. 2*B*). For TNF-$\alpha^{-/-}$→WT animals, some macrophages (Fig. 2*C*) stain positive for TNF-α (Fig. 2*D*), whereas the majority lacks TNF-α. Also F4/80-negative but TNF-α-positive cells are detected. Based on the morphology, these cells are mature adipocytes. Whereas in TNF-$\alpha^{+/+}$→KO animals most F4/80-positive cells are TNF-α positive (Fig. 2, *E* and *F*, respectively), some lack TNF-α (Fig. 2, *G* and *H*). In the epididymal fat pad of TNF-$\alpha^{-/-}$→KO animals, no TNF-α was detected (Fig. 2, *I* and *J*).

Table 2. *Obesity/inflammatory markers in epididymal fat*

Genotype	Relative Amount of mRNA (Fold)			
	F4/80	*P*	Leptin	*P*
TNF-$\alpha^{+/+}$→WT (control)	1.1±0.1	0.66	1.1±0.1	0.14
TNF-$\alpha^{-/-}$→WT	1.0±0.1		0.8±0.1	
TNF-$\alpha^{-/-}$→KO (control)	1.2±0.3	0.01	1.1±0.2	0.001
TNF-$\alpha^{+/+}$→KO	3.3±0.7		2.7±0.4	

Values are expressed as means ± SE; n = 7–8 experiments. *P* values are for the comparison as indicated in the table.

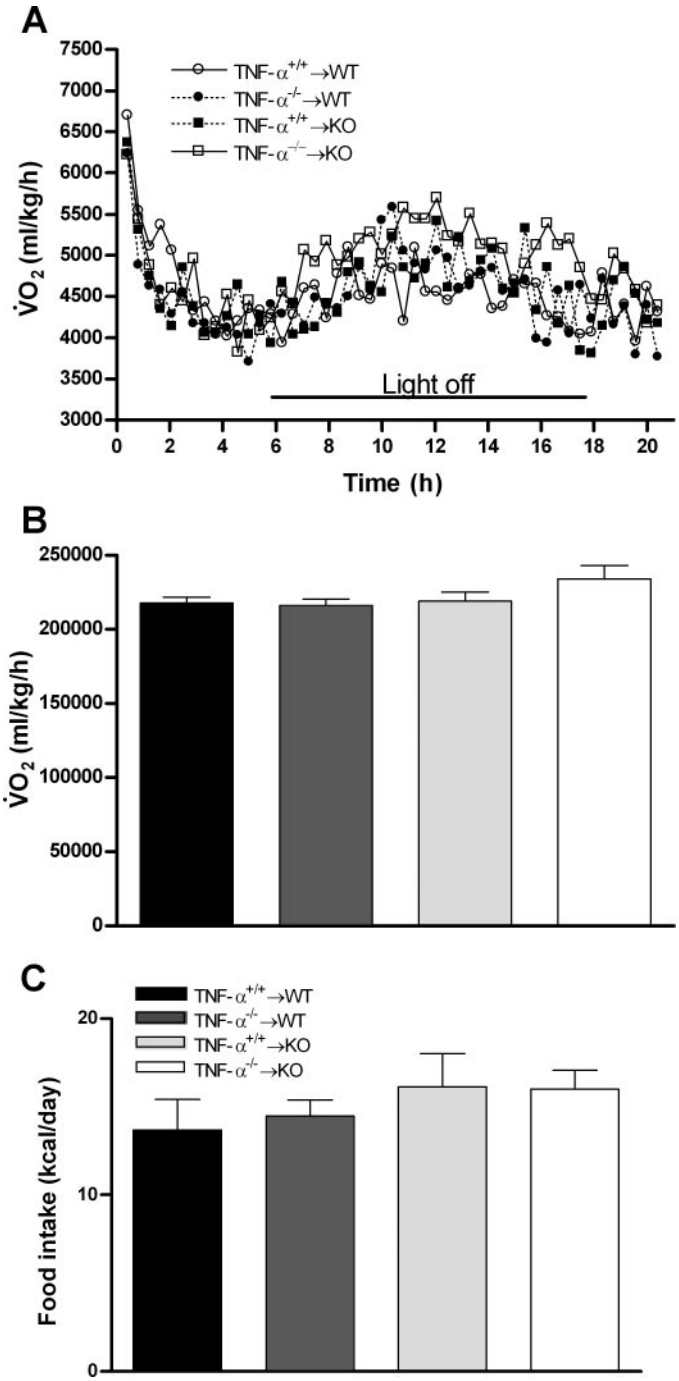

Fig. 4. Macrophage TNF-α does not alter metabolic rate or food intake. *A* and *B*: no differences were seen for oxygen consumption for WT hosts and KO hosts, respectively ($P > 0.05$ for both comparisons; n = 7–8). *C*: food intake was similar for all groups ($P > 0.05$ for both KO and WT hosts; n = 7–8, each measurement is the average of 3 individual measurements). Data are expressed as means ± SE.

Macrophage TNF-α influences the development of obesity and inflammation. The absence or presence of TNF-α in bone marrow donor and/or host did not influence relative weight gain to a significant extent, even though TNF-$\alpha^{-/-}$→KO mice tended to gain less weight (Fig. 3*A*; $n = 7–8$). There were no significant differences between groups ($P = 0.2$) in terms of relative weight gain; no bone marrow-derived effect was apparent ($P = 0.67$ and $P = 0.2$ for the WT host and the KO host combinations, respectively). The age-matched KO littermates had a slightly lower initial weight compared with the age-matched WT littermates, in agreement with the strain description by Jackson Laboratory. This corresponded with a difference in the final weights after 26 wk on the HFD (Table 1). Therefore, and because the WT mice are not littermates with the KO mice, and since the main interest of the current study lies in the importance of macrophage TNF-α, we focused on a potential effect of donor TNF-α genotype within the same host group.

TNF-α influences the size of the epididymal fat pad (Fig. 3*B*; $n = 7–8$). Figure 3*B* suggests that bone marrow donor genotype contributes to the difference in epididymal fat pad size, with both groups receiving TNF-$\alpha^{+/+}$ bone marrow exhibiting greater epididymal fat weight than their counterparts receiving TNF-$\alpha^{-/-}$ marrow ($P = 0.003$ and 0.02 for the marrow effect in WT and KO hosts, respectively). Body composition data were in agreement with the relative weight gain. Whereas the TNF-$\alpha^{-/-}$→KO mice had the highest relative lean mass ($P < 0.0001$; $n = 7–8$; Fig. 3*C*), they also had the lowest relative total adipose mass ($P < 0.0001$; Fig. 3*D*). Whereas no impact of macrophage TNF-α was seen in the WT hosts ($P = 0.2$ for both relative lean and adipose mass), an effect of bone marrow genotype on both relative lean and adipose mass was seen on the TNF-α-deficient background ($P = 0.004$ for both). The levels of expression of F4/80 mRNA were quantified as an index of the accumulation of inflammatory cells (macrophages) in the epididymal fat pad (Table 2). Leptin mRNA levels, indicative of both obesity and inflammation, were in agreement with the F4/80 data: an effect of marrow TNF-α genotype was seen for KO hosts; no impact was observed in the WT hosts (Table 2). No differences were observed in the ratio of stromal cells/adipocytes (data not shown). Adipocyte size was slightly larger for TNF-$\alpha^{+/+}$→WT mice [4,251 ± 360, 2,593 ± 485, 3,522 ± 205, and 3,496 ± 301 μm^2 for WT hosts receiving TNF-$\alpha^{+/+}$ and TNF-$\alpha^{-/-}$ and KO hosts receiving TNF-$\alpha^{+/+}$ and TNF-$\alpha^{-/-}$ bone marrow, respectively ($n = 5$; $P = 0.03$)].

Analysis of the metabolic rate showed no difference between groups in $\dot{V}O_2$ when comparing oxygen use per kilogram lean weight over time ($P = 0.7$ and 0.2 for WT and KO hosts, respectively; $n = 7–8$; Fig. 4*A*). Total oxygen utilization used during the 20-h period tended to be higher for TNF-$\alpha^{-/-}$→KO, as reflected by the total area under the curve; however, this did not reach statistical significance ($P = 0.8$ and 0.2 for WT and KO hosts, respectively; Fig. 4*B*). This is in agreement with the trend seen for relative weight gain. Food intake was comparable for the different groups ($P = 0.6$; Fig. 4*C*) No differences were seen in terms of mobility ($P = 0.1$) or respiratory exchange ratio ($P = 0.1$; data not shown).

Macrophage TNF-α influences insulin sensitivity. Euglycemic-hyperinsulinemic clamp studies were performed on conscious mice to determine the insulin sensitivity ($n = 7–8$ for all analysis; Fig. 5, *A–D*). Plasma glucose levels measured between *minute 80* and *120* were comparable for the four groups ($P = 0.8$; Fig. 5*B*), whereas the glucose infusion rates (GIR) were significantly different ($P = 0.0006$; Fig. 5*D*). The KO hosts receiving TNF-$\alpha^{-/-}$ bone marrow exhibited higher insulin sensitivity compared with the TNF-$\alpha^{+/+}$→KO animals (GIR = 43.8 ± 2.8 vs. 28.3 ± 3.2 $mg \cdot kg^{-1} \cdot min^{-1}$, respectively; $P = 0.004$); no difference was seen for the WT hosts (GIR = 21.3 ± 3.7 vs. 28.2 ± 5.0 $mg \cdot kg^{-1} \cdot min^{-1}$ for TNF-$\alpha^{+/+}$→WT vs. TNF-$\alpha^{-/-}$→WT, respectively; $P = 0.3$). To exclude that the difference in insulin sensitivity was the result of the small, but not significant, difference in weight for KO hosts (Table 1), four weight-matched animals from each group of the KO hosts were compared (supplemental Fig. 1; Supplemental data for this article are available online at the *American Journal of Physiology-Endocrinology and Metabolism* website). The GIR were comparable with the ones for all KO animals (GIR = 47.0 ± 5.0 vs. 27.7 ± 2.9 $mg \cdot kg^{-1} \cdot min^{-1}$ for TNF-$\alpha^{-/-}$→KO and TNF-$\alpha^{+/+}$→KO, respectively; $P = 0.008$). In agreement with the insulin sensitivity, fasting plasma insulin levels after 26 wk on a HFD were significantly different for the KO hosts ($P = 0.002$; Fig. 5*E*). No difference was seen for the WT hosts ($P = 0.7$). Fasting plasma glucose values tended to be higher for TNF-$\alpha^{+/+}$→KO vs. TNF-$\alpha^{-/-}$→KO animals (244 ± 18 vs. 188 ± 21 mg/dl, respectively; $P = 0.06$). No difference was seen for the WT hosts (176 ± 23 vs. 172 ± 27 mg/dl for the group receiving TNF-$\alpha^{+/+}$ and TNF-$\alpha^{-/-}$, respectively; $P = 0.9$). Before the start of the HFD, both fasting plasma glucose ($P = 0.7$ and 0.8 for WT and KO hosts, respectively) and fasting insulin levels ($P = 0.7$ and 0.3 for the WT and KO hosts, respectively) did not differ. Overall, the data are indicative for the development of a different degree of insulin resistance. Average islet size, while showing a wide variability in size within each group, generally corresponded with the insulin sensitivity data (20,108 ± 9,752, 20,544 ± 11,347, 10,069 ± 4,027, and 11,572 ± 2,440 μm^2 for the WT and KO hosts receiving TNF-$\alpha^{+/+}$ and TNF-$\alpha^{-/-}$ marrow, respectively; $P > 0.05$ for the comparison within each host group).

Determination of the whole body glucose turnover was in agreement with the insulin sensitivity (Fig. 5*F*). Whereas no impact of macrophage TNF-α is visible in WT hosts ($P = 0.3$), a detrimental effect is seen for KO hosts ($P = 0.04$). Glucose clearance followed the same trend (Fig. 5*G*), however, without reaching statistical significance for both WT and KO hosts ($P > 0.5$ for both WT and KO hosts). Finally, endogenous glucose production generally corresponded with insulin sensitivity (Fig. 5*H*), even though the impact of different bone marrow did again not reach statistical significance ($P > 0.05$ for both WT and KO hosts). No differences were observed for each of these measurements before the start of the insulin

Fig. 5. Macrophage TNF-α influences insulin sensitivity in TNF-$\alpha^{-/-}$ animals. *A–D*: plasma glucose levels ($P > 0.05$ for both WT and KO hosts; *A* and *B*) and glucose infusion rates (GIR; $*P = 0.004$; *C* and *D*) were determined during euglycemic-hyperinsulinemic clamp studies. *E*: plasma insulin levels ($*P = 0.002$) at the end of the 26-wk diet. *F*: whole body glucose turnover ($*P = 0.02$). *G* and *H*: clearance (*G*) and endogenous glucose production (*H*) were in agreement with the GIR. Data are expressed as means ± SE; $n = 7–8$.

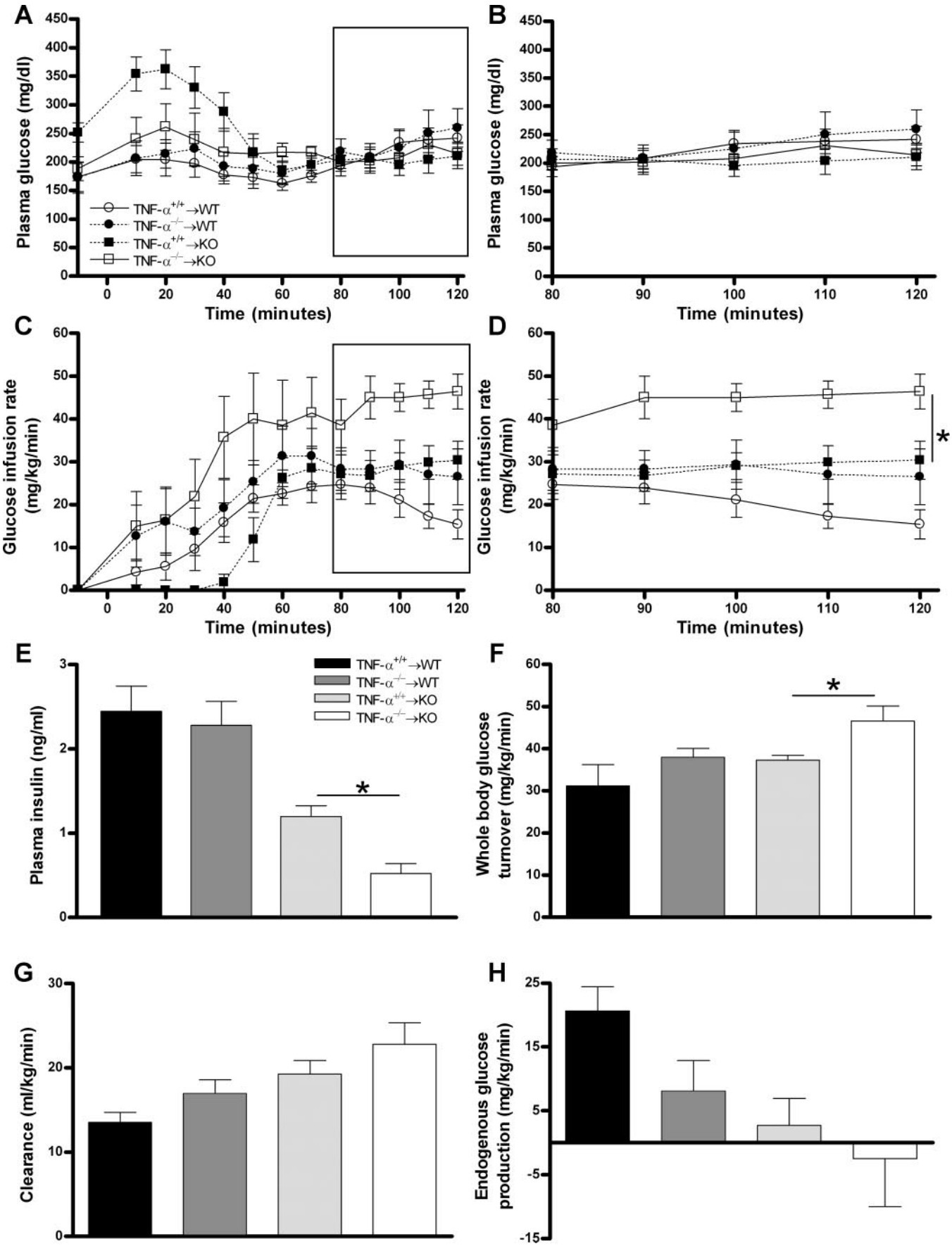

infusion ($t = -10$ min; supplemental Table 1; Supplemental data for this article are available online at the *American Journal of Physiology: Endocrinology and Metabolism* website.).

Glucose uptake was determined in muscle (soleus, gastrocnemius, and vastus), adipose tissue, diaphragm, heart, and brain ($n = 6–8$). As expected, there were no differences between groups with respect to brain uptake ($P > 0.05$ for both WT and KO hosts). Uptake in the heart and diaphragm was also not different between groups ($P > 0.05$ for each organ for both WT and KO hosts; data not shown). Glucose uptake in muscle (soleus, gastrocnemius, and vastus) did not show any difference either ($P > 0.05$ for WT and KO hosts; data not shown). However, the glucose uptake in adipose tissue generally showed a trend corresponding with insulin sensitivity. The presence of TNF-α in the bone marrow tended to reduce glucose uptake in the epididymal fat pad of KO hosts (10 ± 3 vs. 15 ± 9 mg·min^{-1}·kg^{-1} for TNF-α$^{+/+}$→KO and TNF-α$^{-/-}$→KO, respectively; $P = 0.6$), whereas no difference was observed in WT hosts (3 ± 0.5 mg·min^{-1}·kg^{-1} independent of marrow; $P = 1$).

Macrophage TNF-α influences hepatic lipid accumulation. Livers from the different groups differed in weight ($n = 7–8$; Fig. 6*A*). Whereas macrophage TNF-α did not influence liver weight in WT hosts ($P = 0.2$), the TNF-α$^{+/+}$ marrow in KO mice led to a significant increase in liver weight ($P = 0.03$). Considering the reported impact of TNF-α on NAFLD and NASH, hematoxylin/eosin staining was performed on liver tissue (Fig. 7, *A* and *C*). The livers from TNF-α$^{-/-}$→KO mice were protected from diet-induced fatty liver changes (Fig. 7). The presence of lipid droplets in the liver tissue was ascertained by Oil red O staining and was indicative of less fat in TNF-α$^{-/-}$→KO (Fig. 7*B*). Livers from TNF-α$^{+/+}$→WT, TNF-α$^{-/-}$→WT, and TNF-α$^{+/+}$→KO animals showed no protection against lipid accumulation and looked similar as those shown in Fig. 7, *C* and *D*. This was confirmed by analysis of the liver lipid content ($n = 5$; Fig. 8). No differences were observed for cholesteryl esters and unesterified cholesterol. Livers from TNF-α$^{-/-}$→KO mice showed slightly higher phospholipid levels when compared with the other groups ($P = 0.02$). However, when comparing TNF-α$^{+/+}$→KO with TNF-α$^{-/-}$→KO livers, the difference was not significant ($P = 0.06$). Triglyceride levels differed among the various groups ($P = 0.001$; Fig. 8*D*). The presence of TNF-α in bone marrow-derived cells is sufficient to lead to triglyceride accumulation in KO hosts ($P = 0.002$). Finally, the absence of lipid accumulation in the TNF-α$^{-/-}$→KO mice corresponded with a reduced rate of inflammation, as indicated by CD68 mRNA levels ($P = 0.03$; $n = 7–8$; Fig. 6*B*) and F4/80 mRNA levels, a more specific macrophage marker then CD68 ($P = 0.03$; $n = 7–8$; Fig. 6*C*). No differences were seen for the WT hosts ($P > 0.05$ for both CD68 and F4/80 mRNA levels; data not shown).

Liver glycogen content was comparable for the different host/donor combinations (data not shown; $P > 0.05$ for both WT and KO hosts).

TNF-α and lipid homeostasis. TNF-α can influence insulin sensitivity through a variety of pathways, eventually leading to differences in lipogenesis and/or lipolysis. Considering the difference in visceral fat pad weight and the different

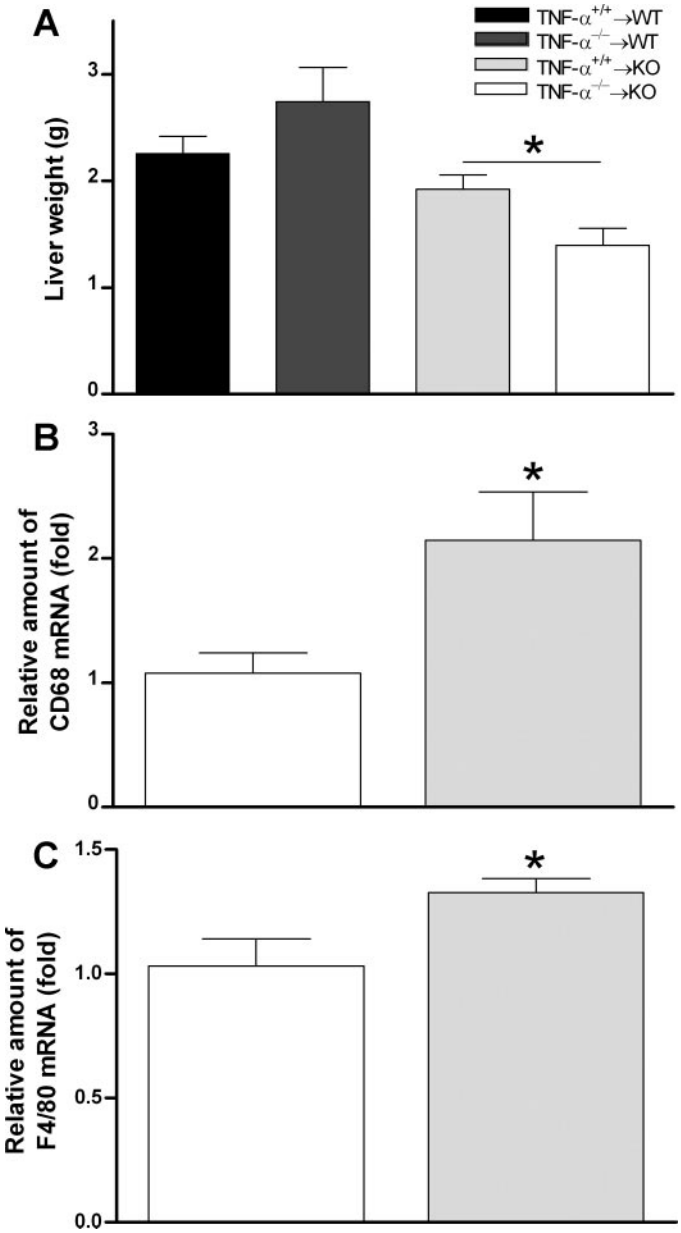

Fig. 6. The liver is an important target for macrophage TNF-α. Liver weight (*$P = 0.03$; *A*), CD68 mRNA levels (*$P = 0.03$; *B*), and F4/80 mRNA levels (*$P = 0.03$; *C*) were significantly different for the TNF-α$^{+/+}$→KO relative to TNF-α$^{-/-}$→KO animals. Data are expressed as means ± SE; $n = 7–8$.

degree of liver steatosis, we measured mRNA levels of a variety of metabolic markers in adipose tissue and liver, focusing on lipogenesis/lipolysis ($n = 7–8$; supplemental Table 2).

To determine the cause of triglyceride accumulation in the liver, we investigated potential differences in triglyceride oxidation and production. No differences were seen for mRNA levels of peroxisome proliferator-activated receptor (PPAR)α (an important mediator of triglyceride oxidation), or glycerol-3-phosphate dehydrogenase (a PPARα-mediated enzyme involved in the conversion from glycerol to glucose). mRNA levels of protein phosphatase 2C, shown to be upregulated by TNF-α and to reduce acetyl-CoA carboxylase (ACC) phosphorylation, finally leading to reduced fatty acid oxidation

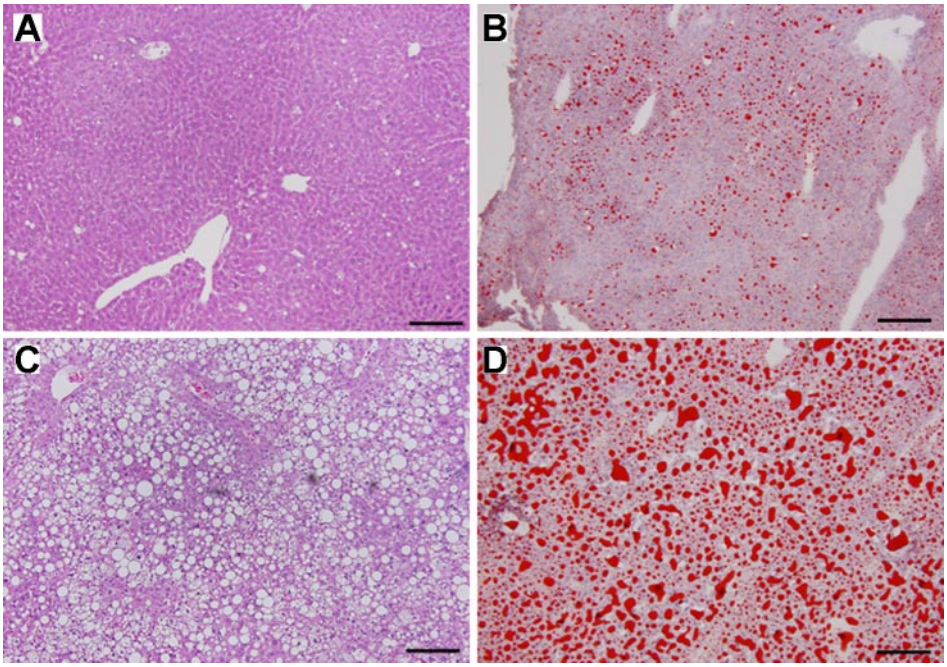

Fig. 7. Macrophage TNF-α influences hepatic lipid accumulation. Hematoxylin/eosin staining (*A* and *C*) and Oil red O staining (*B* and *D*) revealed the deleterious effect of macrophage TNF-α in the livers from TNF-$\alpha^{+/+}$→KO (*C* and *D*) vs. TNF-$\alpha^{-/-}$→KO animals (*A* and *B*).

(39), were not influenced by macrophage TNF-α ($P = 0.5$ and 0.7 for KO and WT hosts, respectively). Furthermore, no difference was seen for lipoprotein lipase (LPL) mRNA, suggesting that the difference in triglyceride level (Fig. 8*D*) is the consequence of a difference in de novo synthesis and not in uptake. Levels of PPARγ mRNA, associated with lipogenesis, were in agreement with the different degree of fat accumulation in the liver. Whereas no difference was observed for WT hosts ($P = 0.45$), PPARγ mRNA levels were 1.9-fold higher in TNF-$\alpha^{+/+}$→KO vs. TNF-$\alpha^{-/-}$→KO animals ($P = 0.006$). Levels of aP2 mRNA (fatty acid-binding protein typical for adipocytes) were also increased 1.9-fold in TNF-$\alpha^{+/+}$→KO vs. TNF-$\alpha^{-/-}$→KO animals ($P = 0.01$), with no difference for the WT hosts ($P = 0.09$). This is an interesting observation, since it has been reported that an increase in liver PPARγ levels can lead to adipogenic hepatic steatosis (50). With regard to fatty acid production, we quantified mRNA for two key enzymes of fatty acid synthesis, i.e., ACC, which catalyzes the synthesis of malonyl-CoA, and fatty acid synthase (FAS), a multifunctional protein that synthesizes fatty acids by adding malonyl-CoA units to an acetyl-CoA primer. mRNA levels of FAS were significantly different for the KO hosts, with a 2.4-fold increase for TNF-$\alpha^{+/+}$→KO vs. TNF-$\alpha^{-/-}$→KO animals ($P = 0.001$). This was in agreement with a twofold increase in mRNA levels for ACC for TNF-$\alpha^{+/+}$→KO animals ($P = 0.003$). No difference was seen for the WT hosts ($P = 0.6$ and 0.3 for FAS and ACC mRNA, respectively). mRNA levels of SOCS-3, known to be upregulated by TNF-α and to increase ACC and FAS mRNA levels through suppression of STAT3 phosphorylation (43), showed a similar profile, whereas no difference was seen for the WT hosts ($P = 0.9$); SOCS-3 mRNA levels in TNF-$\alpha^{+/+}$→KO livers were twofold increased vs. TNF-$\alpha^{-/-}$→KO livers ($P = 0.03$). Western blot analysis did not reveal an effect of macrophage TNF-α on STAT3 protein levels or STAT3 phosphorylation in KO hosts (data not shown). Although other pathways are potentially involved, it cannot be excluded that the lack of a difference is because of the insensitivity of the method. Unexpectedly, no difference was seen for SREBP-1 mRNA levels. In addition to SREBP-1 and PPARγ, liver mRNA levels for ChREBP-1, a third major lipogenic transcription factor, were analyzed. No differences were observed between groups.

Expression levels of glucose-6-phosphatase, determined by RT-QPCR, were 2.2-fold higher in TNF-$\alpha^{+/+}$→KO vs. TNF-$\alpha^{-/-}$→KO animals ($P = 0.01$), whereas no difference was seen for WT hosts ($P = 0.5$). Liver mRNA levels of glucokinase were not altered by the bone marrow genotype ($P = 0.4$ and 0.8 for WT and KO hosts, respectively). The trend for improved insulin suppression of endogenous glucose output (Fig. 5*H*) may reflect an improved suppression of gluconeogenesis, since tracer incorporation in liver glycogen was unaffected (data not shown; $P = 0.95$). Interestingly, levels of phospho*enol*pyruvate kinase showed no difference.

In the epididymal fat pad, no differences were seen for PPARγ, hormone-sensitive lipase (HSL), LPL, SREBP-1 or ChREBP-1 mRNA levels. In agreement with previous data from Kirchgessner et al. (22), leptin mRNA levels were 2.5-fold higher in TNF-$\alpha^{+/+}$→KO vs. TNF-$\alpha^{-/-}$→KO animals ($P = 0.002$), with no difference for WT hosts ($P = 0.1$). In agreement with a previous study (11), SOCS-3 showed an expression profile similar to that seen in the livers: mRNA levels were 2.2-fold higher in TNF-$\alpha^{+/+}$→KO vs. TNF-$\alpha^{-/-}$→KO animals ($P = 0.02$), whereas no difference was seen for the WT hosts ($P = 0.1$). The differences in SOCS-3 levels were not associated with changes in FAS or ACC mRNA.

The data indicate that the presence of TNF-α in macrophages is sufficient to cause insulin resistance, adipose tissue expansion, and fatty liver disease in TNF-$\alpha^{-/-}$ animals. However, lack of differences in analyzed parameters for the WT hosts indicate that host TNF-α contributes significantly to the "metabolic syndrome phenotype." Because SOCS-3 mRNA levels were

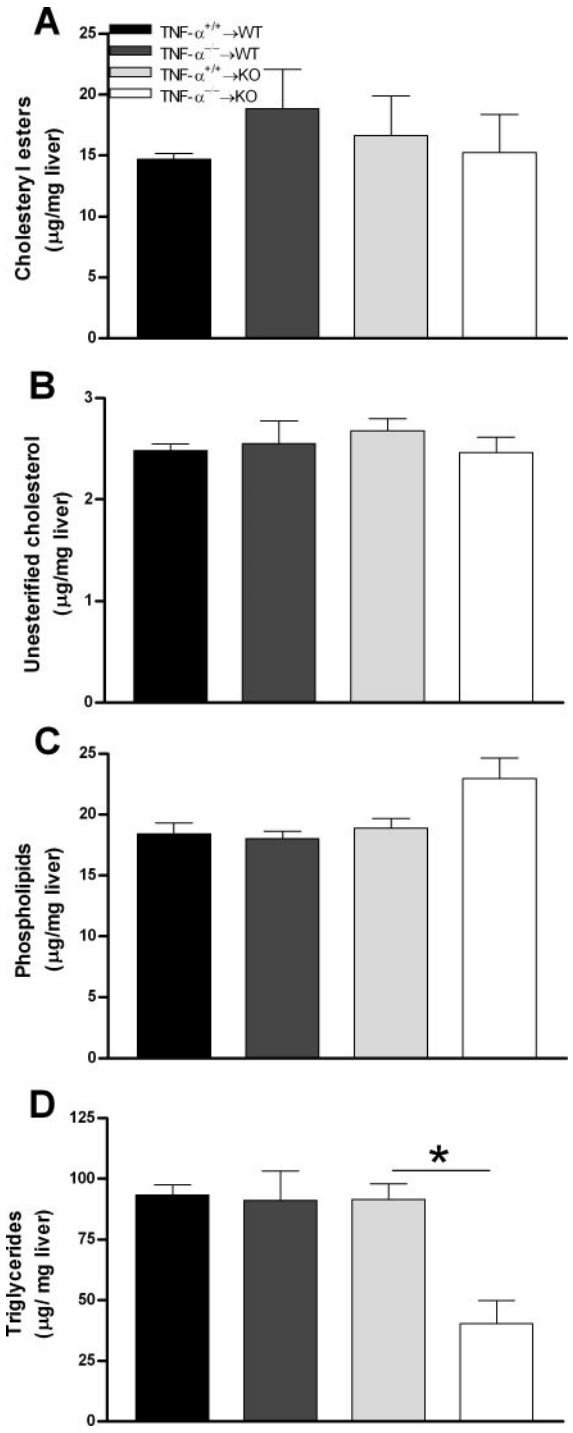

Fig. 8. Macrophage TNF-α increases liver triglyceride levels in TNF-$\alpha^{-/-}$ animals. Although no differences were observed for hepatic cholesteryl esters, unesterified cholesterol, and phospholipid levels (*A–C*), triglyceride levels were different for the KO hosts (*$P = 0.002$; *D*). Data are expressed as means ± SE; $n = 5$.

altered in the KO hosts in both liver and adipose tissue, we measured interleukin (IL)-6 mRNA levels, since it has been shown that TNF-α and IL-6 exert similar effects through SOCS-3 activation (36). No differences were observed for either liver or adipose tissue IL-6 expression for WT or KO hosts (supplemental Table 2).

DISCUSSION

More than 64% of U.S. adults are either overweight or obese, according to results from the 1999–2000 National Health and Nutrition Examination Survey (14). Because obesity is associated with evidence of systemic inflammation and promotes an increased risk of diabetes mellitus and NAFLD, a better understanding of the contribution of inflammatory cells and their inflammatory cytokines in the development of obesity and its consequences is critical. Cytokines such as TNF-α have been shown to lead to impaired glucose homeostasis and fatty liver disease. Several cell types, such as adipocytes and macrophages, are involved in the production of this cytokine, with the vast majority of the inflammatory gene transcripts being expressed in cells from the stromal-vascular fraction of adipose tissue (7). The number of visceral fat macrophages is increased in rodent models of obesity (47, 48) and positively correlated to the body mass index in humans (7, 9). In liver, macrophages are considered to be the most important source of TNF-α (40). Therefore, we hypothesized that TNF-α produced by bone marrow cells would impact the development of insulin resistance and fatty liver disease in the setting of diet-induced obesity.

Both TNF-α WT and KO mice were transplanted with either TNF-$\alpha^{+/+}$ or TNF-$\alpha^{-/-}$ bone marrow and fed a HFD for 26 wk. As expected, bone marrow-derived cells are the predominant source of TNF-α in adipose tissue (85%) and in the liver (75%). Skeletal muscle tissue has been shown to produce increased amounts of TNF-α in insulin-resistant and diabetic patients (35) but, even though the percentage of macrophages in the adipose tissue that surrounds and infiltrates skeletal muscle increases in obese mice compared with lean mice (33, 35), our data indicate that bone marrow-derived cells lead to a minor contribution in TNF-α production in skeletal muscle of obese mice. The higher levels of TNF-α mRNA in adipose tissue of TNF-$\alpha^{+/+}$→KO vs. TNF-$\alpha^{+/+}$→WT mice might be explained by the absence of negative-feedback mechanisms in the KO hosts, since these animals were never exposed to the cytokine during development.

Relative weight gain did not differ among the four groups of mice, although TNF-$\alpha^{-/-}$→KO mice tended to gain less weight. However, the size of the epididymal fat pad varied significantly. This is in agreement with data from Uysal et al. (45) showing that both TNF-α KO and WT mice develop obesity when fed a HFD for 12 wk, with KO mice exhibiting a tendency to gain less weight over time. Furthermore, this finding, together with the trend for an increased metabolic rate in TNF-$\alpha^{-/-}$→KO mice, is in agreement with a potential role for TNF-α in brown adipose tissue physiology (31).

In the present study, all mice were euglycemic after 26 wk on the HFD. However, the differences in insulin values suggest that TNF-α, produced by cells derived from marrow, provides different degrees of a compensatory response to the development of obesity-induced insulin resistance. This was confirmed by euglycemic-hyperinsulinemic clamp studies. At equilibrium, the GIR necessary to maintain plasma glucose at 200 mg/dl varied among the different groups, with the mice lacking TNF-α showing the highest insulin sensitivity. Based on the different GIR, we infer that KO hosts receiving TNF-$\alpha^{-/-}$ marrow are at least partially protected from the development of insulin resistance when compared with their littermates that

received TNF-$\alpha^{+/+}$ marrow. Interestingly, the absence of TNF-α in bone marrow-derived cells is not sufficient to protect WT animals from insulin resistance. The impact of macrophage TNF-α on insulin sensitivity, as indicated by different GIR, was in agreement with differences in whole body glucose turnover and glucose clearance. Surprisingly, glucose uptake in muscle did not differ between the four groups. A trend was seen for glucose uptake in epididymal fat pad that was in agreement with the insulin sensitivity, as determined by the clamp studies. We hypothesize that, whereas the methods used in this study do not allow detection of organ-specific glucose uptake, they do permit the detection of overall differences in glucose uptake. This may be explained by the fact that the mice are all insulin resistant to a certain degree because of the HFD for 26 wk. Because no animals on standard chow were included in the study, a possible increase in insulin resistance because of diet alone could not be analyzed. Interestingly, in adipose tissue, one of the organs with the most outspoken contribution of bone marrow-derived cells to TNF-α production, differences, even though not significant, are most pronounced. These findings are in agreement with a previous study showing that a dramatic upregulation of macrophage-related genes is mostly restricted to white adipose tissue; mRNA of these genes was barely detectable and essentially unchanged in muscle and liver of obese mice. Furthermore, a significant upregulation of CD68 was observed in the liver after 26 wk on a HFD, although the absolute expression level was much lower than that in fat (48).

The difference in GIR corresponds with the trend in endogenous glucose production, indicative of an important role for the liver in translating the effect of TNF-α on glucose homeostasis. The absence of insulin resistance in the liver of TNF-$\alpha^{-/-}\rightarrow$KO mice agrees with the lower level of glucose-6-phosphatase mRNA compared with the other groups and is indicative of an improved suppression of gluconeogenesis. Furthermore, the livers from TNF-$\alpha^{-/-}\rightarrow$KO mice were protected from diet-induced steatosis. Considering the KO hosts, this clearly indicates an impact of macrophage-derived TNF-α. Even though in physiological conditions hepatocytes are the main site of hepatic glucose metabolism, Kupffer cells are sensitive to insulin-mediated increased glucose utilization (38), and their products have been shown to play a role in the regulation of glucose homeostasis (3). Kupffer cells are the primary source of hepatic TNF-α (40), and their number has been shown to increase in a nutritional model of NASH (41). Our data confirm and extend on these findings.

Hepatic steatosis results from an excessive accumulation of triglycerides in hepatocytes and is influenced by lipogenesis and fatty acid oxidation. Although no differences were seen for genes related to fatty acid oxidation, mRNA levels of PPARγ, one of the lipogenic transcription factors, were significantly lower in mice deficient in TNF-α vs. TNF-$\alpha^{+/+}\rightarrow$KO animals. No difference was observed for WT animals. The difference in PPARγ mRNA levels is indicative for so-called adipogenic steatosis (28, 50). Whereas PPARγ is normally expressed at very low levels in the liver, in animal models with insulin resistance and fatty livers, the expression is markedly increased (5). Similar observations were made for ACC and FAS mRNA, two enzymes involved in fatty acid synthesis. Interestingly, SOCS-3 mRNA, known to upregulate ACC and FAS through suppression of STAT3 phosphorylation, showed a similar profile. These findings are in agreement with an established role for TNF-α as an inducer of SOCS-3 expression (11), suggesting that SOCS-3 may be a key mediator in the development of insulin sensitivity and fatty liver disease during inflammation. Although it would be expected that SOCS-3 upregulates SREBP-1, an important lipogenic transcription factor, we did not see a difference in SREBP-1 mRNA levels. A difference in protein level or cleaved, activated form of SREBP-1 could be associated with the observed difference in liver steatosis. However, no difference was detected (data not shown). Because no differences were observed for LPL mRNA levels, it can be concluded that the difference in lipid accumulation is the consequence of de novo fatty acid synthesis and not of uptake of circulating molecules. This is also in agreement with the fact that no differences were observed for mRNA levels of LPL and HSL in adipose tissue. Finally, because IL-6 is known to exert effects similar to those of TNF-α, partially also mediated by SOCS-3, we quantified IL-6 mRNA levels in fat and liver. No differences were observed.

The present study indicates that macrophage TNF-α is important for the development of insulin resistance and NAFLD in TNF-$\alpha^{-/-}$ animals in the setting of obesity. Indeed, whereas most parameters measured in our study were significantly different when comparing KO hosts receiving either TNF-$\alpha^{+/+}$ or TNF-$\alpha^{-/-}$ marrow, this is not the case for the WT hosts. Although this may be partially explained by considerations with respect to sample size, statistical power, and higher variability for the WT F_2 littermates (37), it is more likely to be indicative of the role of host TNF-α, attenuating the differences for the WT hosts. Indeed, considering for example the potential role of TNF-α in cross talk between adipocytes and macrophages (48), low levels of TNF-α could lead to a variety of changes in other markers involved in insulin resistance and inflammation in general and could be sufficient to regulate Kupffer cell activation through paracrine mechanisms (23). Similarly, our laboratory has previously shown that plasminogen activator inhibitor (PAI)-1-deficient animals are partially protected from the development of obesity, an effect that is ablated by simply reconstituting these animals with PAI-$1^{+/-}$ marrow (10). This study and the current study suggest that low cytokine/adipokine levels in the microenvironment are sufficient to initiate paracrine cross talk. Remarkably, transplantation of TNF-α complete or deficient marrow "generated" a liver and adipose phenotype with no effect on muscle. Even though these findings differ with previous work (45), it might be related to a different degree of insulin resistance because of differences in factors such as diet composition and length of feeding period. In support of this assumption, previous studies using models of hyperphagia [gold-thioglucose injection (46) and *ob/ob* mice (45)] also lead to different conclusions, mainly concerning the differences in body weight, fat pad weight, and percent body fat, and are furthermore not completely in agreement with each other. However, all studies are consistent in reporting increased insulin sensitivity for TNF-α deficient mice. In addition, it cannot be excluded that the irradiation procedure itself led to some discrepancies with respect to previous studies. With regard to the bone marrow transplantation, it has been shown that high-fat feeding promotes the trafficking of bone marrow-derived circulating progenitor cells to adipose tissue and their differentiation in multilocular adipocytes (8). Therefore, it cannot be excluded

that newly recruited adipocytes, or other bone marrow-derived cells in general, contribute to our observations. However, no multilocular adipocytes were detected, nor were there a lot of TNF-α-positive cells that were not F4/80 positive in the epididymal fat pad of TNF-$\alpha^{+/+}\rightarrow$KO animals. Finally, our data indicate that the absence of TNF-α protects at least partially from the development of obesity, as reflected by the epididymal fat pad weight. This might explain the observed difference in liver phenotype. However, considering the changed expression levels of the different liver enzymes in combination with other studies suggesting a direct impact of TNF-α on the development of fatty liver disease, we hypothesize at least a partial direct local role for Kupffer cell-derived TNF-α on the development of NAFLD.

In conclusion, our study is the first to discriminate a separate inflammatory cell-mediated TNF-α effect. The results indicate the significant contribution of inflammation-mediated TNF-α production for the development of fat accumulation, insulin resistance, and fatty liver disease. However, the study also clearly indicates an at least as important role for host TNF-α.

ACKNOWLEDGMENTS

We thank the Mouse Metabolic Phenotyping Center at Vanderbilt University for the use of the Minispec and Oxymax indirect calorimeter and help with the liver lipid quantification (U24 DK59637). Furthermore, we thank C. Malabanan, A. Wilson, T. Ansari and T. Santomango for the training and assistance with the clamp studies and glycogen analysis and Dr. O. McGuinness for time and valuable input for the data interpretation.

GRANTS

This study was supported by National Heart, Lung, and Blood Institute Grants HL-51387, P50HL-081089, and HL-65192.

REFERENCES

1. **Ayala JE, Bracy DP, McGuinness OP, Wasserman DH.** Considerations in the design of hyperinsulinemic-euglycemic clamps in the conscious mouse. *Diabetes* 55: 390–397, 2006.
2. **Beutler B, Cerami A.** Cachectin (tumor necrosis factor): a macrophage hormone governing cellular metabolism and inflammatory response. *Endocr Rev* 9: 57–66, 1988.
3. **Casteleijn E, Kuiper J, van Rooij HC, Kamps JA, Koster JF, van Berkel TJ.** Hormonal control of glycogenolysis in parenchymal liver cells by Kupffer and endothelial liver cells. *J Biol Chem* 263: 2699–2703, 1988.
4. **Chan TM, Exton JH.** A rapid method for the determination of glycogen content and radioactivity in small quantities of tissue or isolated hepatocytes. *Anal Biochem* 71: 96–105, 1976.
5. **Chao L, Marcus-Samuels B, Mason MM, Moitra J, Vinson C, Arioglu E, Gavrilova O, Reitman ML.** Adipose tissue is required for the antidiabetic, but not for the hypolipidemic, effect of thiazolidinediones. *J Clin Invest* 106: 1221–1228, 2000.
6. **Cinti S, Mitchell G, Barbatelli G, Murano I, Ceresi E, Faloia E, Wang S, Fortier M, Greenberg AS, Obin MS.** Adipocyte death defines macrophage localization and function in adipose tissue of obese mice and humans. *J Lipid Res* 46: 2347–2355, 2005.
7. **Clement K, Viguerie N, Poitou C, Carette C, Pelloux V, Curat CA, Sicard A, Rome S, Benis A, Zucker JD, Vidal H, Laville M, Barsh GS, Basdevant A, Stich V, Cancello R, Langin D.** Weight loss regulates inflammation-related genes in white adipose tissue of obese subjects. *FASEB J* 18: 1657–1669, 2004.
8. **Crossno JT Jr, Majka SM, Grazia T, Gill RG, Klemm DJ.** Rosiglitazone promotes development of a novel adipocyte population from bone marrow-derived circulating progenitor cells. *J Clin Invest* 116: 3220–3228, 2006.
9. **Curat CA, Miranville A, Sengenes C, Diehl M, Tonus C, Busse R, Bouloumie A.** From blood monocytes to adipose tissue-resident macrophages: induction of diapedesis by human mature adipocytes. *Diabetes* 53: 1285–1292, 2004.
10. **De Taeye BM, Novitskaya T, Gleaves L, Covington JW, Vaughan DE.** Bone marrow plasminogen activator inhibitor-1 influences the development of obesity. *J Biol Chem* 281: 32796–32805, 2006.
11. **Emanuelli B, Peraldi P, Filloux C, Chavey C, Freidinger K, Hilton DJ, Hotamisligil GS, Van Obberghen E.** SOCS-3 inhibits insulin signaling and is up-regulated in response to tumor necrosis factor-alpha in the adipose tissue of obese mice. *J Biol Chem* 276: 47944–47949, 2001.
12. **Folch J, Lees M, Sloane Stanley GH.** A simple method for the isolation and purification of total lipides from animal tissues. *J Biol Chem* 226: 497–509, 1957.
13. **Halseth AE, Bracy DP, Wasserman DH.** Overexpression of hexokinase II increases insulinand exercise-stimulated muscle glucose uptake in vivo. *Am J Physiol Endocrinol Metab* 276: E70–E77, 1999.
14. **Hedley AA, Ogden CL, Johnson CL, Carroll MD, Curtin LR, Flegal KM.** Prevalence of overweight and obesity among US children, adolescents, and adults, 1999–2002. *JAMA* 291: 2847–2850, 2004.
15. **Hotamisligil GS.** Inflammatory pathways and insulin action. *Int J Obes Relat Metab Disord* 27, *Suppl* 3: S53–S55, 2003.
16. **Hotamisligil GS.** The irresistible biology of resistin. *J Clin Invest* 111: 173–174, 2003.
17. **Hotamisligil GS, Arner P, Caro JF, Atkinson RL, Spiegelman BM.** Increased adipose tissue expression of tumor necrosis factor-alpha in human obesity and insulin resistance. *J Clin Invest* 95: 2409–2415, 1995.
18. **Hotamisligil GS, Budavari A, Murray D, Spiegelman BM.** Reduced tyrosine kinase activity of the insulin receptor in obesity-diabetes. Central role of tumor necrosis factor-alpha. *J Clin Invest* 94: 1543–1549, 1994.
19. **Hotamisligil GS, Peraldi P, Budavari A, Ellis R, White MF, Spiegelman BM.** IRS-1-mediated inhibition of insulin receptor tyrosine kinase activity in TNF-alpha- and obesity-induced insulin resistance. *Science* 271: 665–668, 1996.
20. **Hotamisligil GS, Shargill NS, Spiegelman BM.** Adipose expression of tumor necrosis factor-alpha: direct role in obesity-linked insulin resistance. *Science* 259: 87–91, 1993.
21. **Hotamisligil GS, Spiegelman BM.** Tumor necrosis factor alpha: a key component of the obesity-diabetes link. *Diabetes* 43: 1271–1278, 1994.
22. **Kirchgessner TG, Uysal KT, Wiesbrock SM, Marino MW, Hotamisligil GS.** Tumor necrosis factor-alpha contributes to obesity-related hyperleptinemia by regulating leptin release from adipocytes. *J Clin Invest* 100: 2777–2782, 1997.
23. **Kitamura K, Nakamoto Y, Akiyama M, Fujii C, Kondo T, Kobayashi K, Kaneko S, Mukaida N.** Pathogenic roles of tumor necrosis factor receptor p55-mediated signals in dimethylnitrosamine-induced murine liver fibrosis. *Lab Invest* 82: 571–583, 2002.
24. **Koistinen HA, Bastard JP, Dusserre E, Ebeling P, Zegari N, Andreelli F, Jardel C, Donner M, Meyer L, Moulin P, Hainque B, Riou JP, Laville M, Koivisto VA, Vidal H.** Subcutaneous adipose tissue expression of tumour necrosis factor-alpha is not associated with whole body insulin resistance in obese nondiabetic or in type-2 diabetic subjects. *Eur J Clin Invest* 30: 302–310, 2000.
25. **Kraegen EW, James DE, Jenkins AB, Chisholm DJ.** Dose-response curves for in vivo insulin sensitivity in individual tissues in rats. *Am J Physiol Endocrinol Metab* 248: E353–E362, 1985.
26. **Li Z, Yang S, Lin H, Huang J, Watkins PA, Moser AB, Desimone C, Song XY, Diehl AM.** Probiotics and antibodies to TNF inhibit inflammatory activity and improve nonalcoholic fatty liver disease. *Hepatology* 37: 343–350, 2003.
27. **Livak KJ, Schmittgen TD.** Analysis of relative gene expression data using real-time quantitative PCR and the 2[-Delta Delta C(T)] method. *Methods* 25: 402–408, 2001.
28. **Matsusue K, Haluzik M, Lambert G, Yim SH, Gavrilova O, Ward JM, Brewer B Jr, Reitman ML, Gonzalez FJ.** Liver-specific disruption of PPARgamma in leptin-deficient mice improves fatty liver but aggravates diabetic phenotypes. *J Clin Invest* 111: 737–747, 2003.
29. **Moller DE.** Potential role of TNF-alpha in the pathogenesis of insulin resistance and type 2 diabetes. *Trends Endocrinol Metab* 11: 212–217, 2000.
30. **Morrison WR, Smith LM.** Preparation of fatty acid methyl esters and dimethylacetals from lipids with boron fluoride–methanol. *J Lipid Res* 5: 600–608, 1964.
31. **Nisoli E, Briscini L, Giordano A, Tonello C, Wiesbrock SM, Uysal KT, Cinti S, Carruba MO, Hotamisligil GS.** Tumor necrosis factor alpha mediates apoptosis of brown adipocytes and defective brown adipocyte function in obesity. *Proc Natl Acad Sci USA* 97: 8033–8038, 2000.

32. **Permana PA, Menge C, Reaven PD.** Macrophage-secreted factors induce adipocyte inflammation and insulin resistance. *Biochem Biophys Res Commun* 341: 507–514, 2006.
33. **Perreault M, Marette A.** Targeted disruption of inducible nitric oxide synthase protects against obesity-linked insulin resistance in muscle. *Nat Med* 7: 1138–1143, 2001.
34. **Rajala MW, Scherer PE.** Minireview: the adipocyte—at the crossroads of energy homeostasis, inflammation, and atherosclerosis. *Endocrinology* 144: 3765–3773, 2003.
35. **Saghizadeh M, Ong JM, Garvey WT, Henry RR, Kern PA.** The expression of TNF alpha by human muscle. Relationship to insulin resistance. *J Clin Invest* 97: 1111–1116, 1996.
36. **Senn JJ, Klover PJ, Nowak IA, Zimmers TA, Koniaris LG, Furlanetto RW, Mooney RA.** Suppressor of cytokine signaling-3 (SOCS-3), a potential mediator of interleukin-6-dependent insulin resistance in hepatocytes. *J Biol Chem* 278: 13740–13746, 2003.
37. **Sigmund CD.** Viewpoint: are studies in genetically altered mice out of control? *Arterioscler Thromb Vasc Biol* 20: 1425–1429, 2000.
38. **Spolarics Z, Ottlakan A, Lang CH, Spitzer JJ.** Kupffer cells play a major role in insulin-mediated hepatic glucose uptake in vivo. *Biochem Biophys Res Commun* 186: 455–460, 1992.
39. **Steinberg GR, Michell BJ, van Denderen BJ, Watt MJ, Carey AL, Fam BC, Andrikopoulos S, Proietto J, Gorgun CZ, Carling D, Hotamisligil GS, Febbraio MA, Kay TW, Kemp BE.** Tumor necrosis factor alpha-induced skeletal muscle insulin resistance involves suppression of AMP-kinase signaling. *Cell Metab* 4: 465–474, 2006.
40. **Su GL.** Lipopolysaccharides in liver injury: molecular mechanisms of Kupffer cell activation. *Am J Physiol Gastrointest Liver Physiol* 283: G256–G265, 2002.
41. **Tomita K, Tamiya G, Ando S, Ohsumi K, Chiyo T, Mizutani A, Kitamura N, Toda K, Kaneko T, Horie Y, Han JY, Kato S, Shimoda M, Oike Y, Tomizawa M, Makino S, Ohkura T, Saito H, Kumagai N, Nagata H, Ishii H, Hibi T.** Tumour necrosis factor alpha signalling through activation of Kupffer cells plays an essential role in liver fibrosis of non-alcoholic steatohepatitis in mice. *Gut* 55: 415–424, 2006.
42. **Torti FM, Dieckmann B, Beutler B, Cerami A, Ringold GM.** A macrophage factor inhibits adipocyte gene expression: an in vitro model of cachexia. *Science* 229: 867–869, 1985.
43. **Ueki K, Kondo T, Tseng YH, Kahn CR.** Central role of suppressors of cytokine signaling proteins in hepatic steatosis, insulin resistance, and the metabolic syndrome in the mouse. *Proc Natl Acad Sci USA* 101: 10422–10427, 2004.
44. **Uysal KT, Wiesbrock SM, Hotamisligil GS.** Functional analysis of tumor necrosis factor (TNF) receptors in TNF-alpha-mediated insulin resistance in genetic obesity. *Endocrinology* 139: 4832–4838, 1998.
45. **Uysal KT, Wiesbrock SM, Marino MW, Hotamisligil GS.** Protection from obesity-induced insulin resistance in mice lacking TNF-alpha function. *Nature* 389: 610–614, 1997.
46. **Ventre J, Doebber T, Wu M, MacNaul K, Stevens K, Pasparakis M, Kollias G, Moller DE.** Targeted disruption of the tumor necrosis factor-alpha gene: metabolic consequences in obese and nonobese mice. *Diabetes* 46: 1526–1531, 1997.
47. **Weisberg SP, McCann D, Desai M, Rosenbaum M, Leibel RL, Ferrante AW Jr.** Obesity is associated with macrophage accumulation in adipose tissue. *J Clin Invest* 112: 1796–1808, 2003.
48. **Xu H, Barnes GT, Yang Q, Tan G, Yang D, Chou CJ, Sole J, Nichols A, Ross JS, Tartaglia LA, Chen H.** Chronic inflammation in fat plays a crucial role in the development of obesity-related insulin resistance. *J Clin Invest* 112: 1821–1830, 2003.
49. **You T, Yang R, Lyles MF, Gong D, Nicklas BJ.** Abdominal adipose tissue cytokine gene expression: relationship to obesity and metabolic risk factors. *Am J Physiol Endocrinol Metab* 288: E741–E747, 2005.
50. **Yu S, Matsusue K, Kashireddy P, Cao WQ, Yeldandi V, Yeldandi AV, Rao MS, Gonzalez FJ, Reddy JK.** Adipocyte-specific gene expression and adipogenic steatosis in the mouse liver due to peroxisome proliferator-activated receptor gamma1 (PPARgamma1) overexpression. *J Biol Chem* 278: 498–505, 2003.